 CMES, vol.16, no.1, pp.15-26, 2006

Boundary Element Stress Analysis of Thin Layered Anisotropic Bodies

Y.C. Shiah[1], Y.C. Lin[1], and C. L. Tan[2]

Abstract: In this paper, the order of singularity of the integrals appearing in the boundary integral equation for two-dimensional BEM analysis in anisotropic elasticity is reduced using integration by parts. The integral containing the traction fundamental solution is then analytically integrated to give an exact formulation for a general element of n-order interpolation of the variables. This allows the integrals to be very accurately evaluated even for very thin, slender bodies without the need for excessively refined meshes as in conventional BEM analysis. Three example problems involving thin, layered materials are presented to demonstrate the veracity and successful implementation of the proposed scheme. The BEM results obtained show very good agreement with those obtained analytically for one, and with those from FEM analysis using the commercial software ANSYS for the other two example problems.

keyword: Boundary element method, Nearly-singular integrals, Thin layered anisotropic bodies.

1 Introduction

Accurate stress analysis of layered material systems is of great importance in the assessment of their structural integrity and performance. These material systems are found in, for example, laminated composites, thin film-substrate systems in electronic devices, protective coatings and adhesive joints. Failure at the interfaces such as de-bonding, as well as in the layers due to excessive stresses under mechanical and thermal loads are important design considerations. The adjoining materials are often non-isotropic and the layers, very thin. Laminated composites, single crystal alloy turbine blades with thermal barrier coatings, and thin, bi-crystals in electronic devices, are examples of thin structures with anisotropic material properties. For such bodies, approximate closed-form solutions for the stresses have been derived for a few, relatively simple cases, see, e.g. [Pagano and Hatfield (1972)], [Kant and Swaminathan (2000)], for composite laminates. It is usually necessary, however, to employ numerical methods to perform the stress analysis of these components. To this end the finite element method (FEM) is the computational tool that is most commonly used. Although the boundary element method (BEM) has been well recognized as a very efficient, alternative numerical tool for linear elastic stress analysis, there is paucity of reported works on thin, layered anisotropic bodies.

Besides the added complexities in anisotropic elasticity when compared to the isotropic case, there are further difficulties in using conventional BEM schemes to analyse thin, slender bodies. They stem from the field solutions which are involved in the analytical formulations of the BEM. These solutions are the fundamental solutions to the governing differential equations and they are mathematically singular. In linear elasticity, they give rise to weakly singular and strongly singular integrals in the displacement-based boundary integral equation (BIE). When the source point is very close to the boundary over which integrations are performed, the integrals in the BIE become nearly singular; their evaluation then poses difficulties if conventional quadrature rules based on simple polynomial representations, such as Gauss-Legendre quadrature, are used. This is true even though the integrals are regular in the strict mathematical sense due to the integrands varying very rapidly within the limits of integration. Such situations arise when calculating the displacements and stresses for interior points close to the boundary of the domain; when parts of the boundary are close to one another as in the case of thin, slender structures; or even when very highly graded meshes are used.

Over the past two decades, much effort has been put into developing schemes to regularize singular, near-singular and hypersingular integrals which arise in various BEM formulations. The schemes may often be broadly cat-

[1] Department of Aerospace Eng. and Systems Eng., Feng Chia University, 100 Wenhwa Road, Seatwen 40, Taichung, Taiwan

[2] Correspondence author, Dept. of Mechanical & Aerospace Engng., Carleton University, Ottawa, Canada K1S 5B6

egorized into those in which the regularization is done prior to, or after, the discretisation of the BIE. All of them aim for accuracy, computational efficiency, generality and simplicity; they have, however, been met with only varying degrees of success. Attempts have also been made to unify the understanding on singular and non-singular integration (see, e.g., [Rosen and Cormack (1994)], [Lutz and Gray (1993)]). Reviews and discussion of these developments have been given by, e.g., Krishnasamy, *et al* (1991), Lutz, *et al* (1991), Huang and Cruse (1993), Tanaka, *et al* (1994), Martin, *et al* (1998), Dominguez (2000).

Several schemes have been proposed for the "regularization" of the nearly-singular integrals. Among them are the special weighted Gauss method by Lutz (1992); the projection transformation method of Hayami (1992) and Hayami and Matsumoto (1994); the semi-analytical approach of Taylor series expansion and singularity subtraction for the kernels as employed by Cruse and Aithal (1993) and Mi and Aliabadi (1996); and the variable/coordinate transformation methods of Jun, *et al* (1985), Telles (1987), Huang and Cruse (1993) and Wu and Lu (1996), with or without element sub-division. Other approaches include the kernel cancellation method by Nakagawa (1993), the auxiliary surface method proposed by Liu, *et al* (1993), the line integral method by Krishnasamy, *et al* (1991), as well as analytically regularizing the boundary integral formulations to eliminate the need to compute the nearly singular integrals, e.g. Sladek and Sladek (1992). Richardson and Cruse (1999) have also derived self-regularized displacement-BIE and stress-BIE; the former being obtained by applying a simple solution corresponding a rigid body motion term to Somigliana's displacement identity, and the latter, by subtracting and adding back the first and second terms of the Taylor's series expansion to the original form of the stress-BIE. Regularization techniques using complex poles have also been presented by Dumont (1994) and Granados and Gallego (2001).

In this paper, regularization using integration by parts is carried out on the weakly singular integral in the BIE for two-dimensional anisotropic elastostatics to reduce the order of the singularity of the integrand. Following this, the integral containing the traction fundamental solution is analytically integrated to give the exact formulation for a general element of n-th order interpolation of the variables. This allows the integrals to be very accurately evaluated even for very thin bodies. The effectiveness and applicability of the proposed scheme are demonstrated by numerical examples.

2 Boundary integral equation for plane anisotropy

It is well established in the BEM literature that the conventional boundary integral equation (BIE) for linear elasticity is an integral constraint equation relating the displacements u_j and tractions t_j at the boundary S of the homogeneous elastic domain. In the absence of body forces and thermal effects, it may be written in indicial notation as

$$C_{ij}\,u_i(P)+\int_S u_i(Q)\,T_{ij}(P,Q)dS = \int_S t_i(Q)\,U_{ij}(P,Q)dS \tag{1}$$

In Eq. (1), the value of $C_{ij}(P)$ depends upon the local geometry of S at the source point P; $U_{ij}(P,Q)$ and $T_{ij}(P,Q)$ represent the fundamental solutions of displacements and tractions, respectively, in the x_i-direction at the field point Q due to a unit load in the x_j-direction at P in a homogeneous infinite plane. The explicit forms of these fundamental solutions for linear elastic, anisotropic materials are given by

$$U_{ij}(P,q) = 2Re\left[[r_{i1}A_{j1}\log z_1 + r_{i2}A_{j2}\log z_2]\right] \tag{2}$$

$$\begin{aligned} T_{1j} &= 2n_1 Re\left[\left[\mu_1^2 A_{j1}/z_1+\mu_2^2 A_{j2}/z_2\right]\right] \\ &\quad -2n_2 Re\left[\left[\mu_1 A_{j1}/z_1+\mu_2 A_{j2}/z_2\right]\right] \\ T_{2j} &= -2n_1 Re\left[\left[\mu_1 A_{j1}/z_1+\mu_2 A_{j2}/z_2\right]\right] \\ &\quad +2n_2 Re\left[\left[A_{j1}/z_1+A_{j2}/z_2\right]\right] \end{aligned} \tag{3}$$

where n_i are the components of the unit outward normal vector at Q, the operator Re[[]] gives the real part of complex variables, and z_i is the generalized complex variable defined in terms of the characteristic roots, μ_ι, and the local coordinates of the field point $Q(x_1, x_2)$, (ζ_1, ζ_2), with origin set at the source point $P(x_{p1}, x_{p2})$ as follows

$$z = (x_1 - x_{p1}) + \mu_(x_2 - x_{p2}) \tag{4}$$

For anisotropic materials, Lekhnitskii (1963) has shown that the four roots, μ_ι, of the following characteristic

equation are complex:

$$a_{11}\mu^4 - a_{16}\mu^3 + (2a_{12}+a_{66})\mu^2 - a_{26}\mu + a_{22} = 0 \qquad (5)$$

where a_{mn} are the elastic compliances of the material. In Eq. (2), r_{mn} are material constants, given by

$$r_{1n} = a_{11}\mu_n^2 + a_{12} - a_{16}\mu_n \quad , \quad r_{2n} = a_{12}\mu_n + a_{22}/\mu_n - a_{26} \qquad (6)$$

Also, in Eqs. (2) and (3), A_{jk} are complex constants that can be obtained by

$$\begin{bmatrix} Im[\![B_1]\!] & Re[\![B_1]\!] & Im[\![B_2]\!] & Re[\![B_2]\!] \end{bmatrix} \begin{bmatrix} Re[\![A_{j1}]\!] \\ Im[\![A_{j1}]\!] \\ Re[\![A_{j2}]\!] \\ Im[\![A_{j2}]\!] \end{bmatrix} = \begin{bmatrix} -1/4\pi\,\delta_{j2} \\ 1/4\pi\,\delta_{j2} \\ 0 \\ 0 \end{bmatrix} \qquad (7)$$

where B_k are given by

$$[B_k] = [i\,\mu_k\; r_{1k}\; r_{2k}]^T \qquad (8)$$

and δ_{jk} is the Kronecker delta.

The numerical solution of Eq. (1), the BIE, typically involves discretising the boundary of the solution domain into, say, M segments or elements, each defined by a certain number of nodes, resulting in a total of N nodes on the boundary. Following the usual interpolation process, for $n^{th}-$order elements, the nodal values of coordinates, displacements, and tractions over each element can be expressed in terms of the local coordinate $\xi \in [-1,1]$ as

$$x_j(\xi) = \sum_{c=1}^{n+1} N^{(c)}(\xi)\, x_j^{(c)}, \quad u_j(\xi) = \sum_{c=1}^{n+1} N^{(c)}(\xi)\, u_j^{(c)}, \quad t_j(\xi) = \sum_{c=1}^{n+1} N^{(c)}(\xi)\, t_j^{(c)} \qquad (9)$$

where $N^{(c)}$ are the shape or interpolation functions of the $n^{th}-$degree; it has the general form

$$N^{(c)}(\xi) = \sum_{m=0}^{n} \alpha_m^{(c)} \xi^m \qquad (10)$$

Equation (10) is for general interpolations and it is valid for any interpolation family, such as Serendipity, Lagrange or Hermite. Substitution of Eqs.(9) and (10) into Eq. (1) results in the discretised form of the BIE,

$$C_{ij}(P^a)\,u_i(P^a) = \sum_{b=1}^{M}\sum_{c=1}^{n+1} {}^b t_i^c \int_{-1}^{1} U_{ij}(P^a, {}^bQ) N^c(\xi) J(\xi) d\xi - \sum_{b=1}^{M}\sum_{c=1}^{n+1} {}^b u_i^c \int_{-1}^{1} T_{ij}(P^a, {}^bQ) N^c(\xi) J(\xi) d\xi \qquad (11)$$

where the superscript a represents the a-th global node of the boundary mesh, b denotes the b-th element, and c is the c-th node of the element. Also in Eq. (11), $J(\xi)$ is the Jacobian transformation along the boundary path from the global Cartesian coordinates to the local coordinateξ. The collocation process as represented by Eq. (11) forms a set of linear algebraic equations in terms of the unknown displacements and tractions at the boundary nodes. These linear algebraic equations may be solved by standard matrix methods, such as Gaussian elimination.

In the evaluation of the integrals, which is usually carried out numerically using Gaussian quadrature, care is taken to distinguish the case when the source point P^a is one of the nodes of the b-th element over which the integration takes place, and the case when it is not. Schemes to deal with the former case, where the integrals become weakly singular or singular, are well established in the BEM literature and will not be discussed further here. It is the formulation for the latter case which is the focus of the present work in what follows, and the successful development of which makes it particularly suitable for analyzing thin, slender bodies.

By substituting the fundamental solutions, Eqs.(2), into Eq. (11), the discretised form of the BIE can be written as

$$\begin{aligned} C_{ij}(P^a)\,u_i(P^a) &= \sum_{b=1}^{M}\sum_{c=1}^{n+1} {}^b t_i^c \int_{-1}^{1} 2Re\left[\left[r_{ik}A_{jk}\log {}^b z_k\right]\right] N^c(\xi) J(\xi) d\xi \\ &- \sum_{b=1}^{M}\sum_{c=1}^{n+1}\sum_{i=1}^{2} {}^b u_i^c \int_{-1}^{1} (-1)^{(i-1)} 2\times \\ &Re\left[\left[\mu_k^{\delta_{1i}} A_{jk}\left(\frac{n_1\mu_k - n_2}{{}^b z_k}\right)\right]\right] N^c(\xi) J(\xi) d\xi \end{aligned} \qquad (12)$$

From Eq.(4), it is evident that when the source point

P is very close to, or approaches the integration element, the generalized local coordinate z_k will approach zero. Under this condition, simple numerical integration schemes, such as Gaussian quadrature will not yield accurate results of the near weakly singular integral with the $\log z_k$term and the nearly singular one with the $1/z_k$ term, in Eq.(12) even though the integrals are, strictly speaking, regular. Figure 1 shows a physical example of when such a situation may arise. It is a thin laminated composite consisting of four dissimilar plies bonded with thin adhesive. Many laminated composites used in engineering structures are even thinner than those shown in the figure. The primary goal of the present work is to develop an expedient scheme to accurately evaluate the nearly singular integrals of the BIE for anisotropic elastostatics.

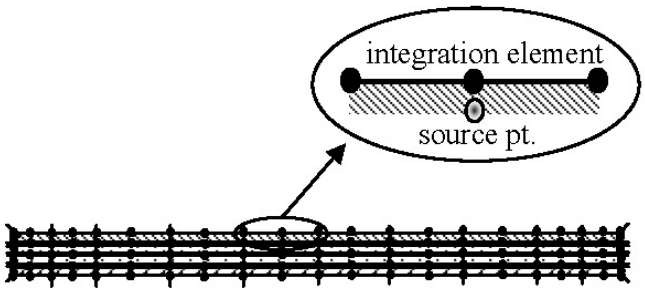

Figure 1 : A thin laminated composite: an example of where nearly singular integral may occur in BEM analysis.

3 Regularization of the integral with the displacement kernel

Typically, the issue of the accurate evaluation of the nearly singular integrals arises when the distance, l, from the source point to the element is one order less than that of the element length. Perhaps the most straightforward approach to resolve the difficulty is to adopt some adaptive scheme which subdivides the element into several sub-intervals so that each sub-interval length becomes the same order as the distance l. Clearly, this is not very practical nor in some instances even feasible for very thin structures. A way to overcome this problem is to analytically reduce the singular integrands into "regular" ones so that the usual numerical integration schemes will give accurate values of the integrals.

First, consider the weakly singular integral term in Eq. (12) involving the displacement fundamental solution (or displacement kernel, for short).

$$\sum_{c=1}^{n+1} {}^b t_i^c \int_{-1}^{1} 2Re\left[\left[r_{ik}A_{jk}\log {}^b z_k\right]\right] N^c(\xi)J(\xi)d\xi \tag{13}$$

With coordinate interpolation, the generalized coordinate $z_k(\xi)$ and the Jacobian $J(\xi)$ may be expressed as

$${}^b z_k = \sum_{m=0}^{n} B_{mk}\xi^m - ({}^b x_{p_1} + \mu_k {}^b x_{p_2}) \tag{14}$$

$$J(\xi) = \sqrt{\begin{array}{l}\left(\sum\limits_{c=1}^{n+1}\sum\limits_{m=1}^{n} m\alpha_m^{(c)}\xi^{m-1}x_1^{(c)}\right)^2 \\ +\left(\sum\limits_{c=1}^{n+1}\sum\limits_{m=1}^{n} m\alpha_m^{(c)}\xi^{m-1}x_2^{(c)}\right)^2\end{array}} \tag{15}$$

where the coefficient B_{mk} is given by

$$B_{mk} = \sum_{c=1}^{n+1} \alpha_m^{(c)}({}^b x_1^{(c)} + \mu_k {}^b x_2^{(c)}) \tag{16}$$

In Eqs. (15) and (16), the superscript (c) denotes the c-th node of the integration element. By substituting Eqs.(10) and (14) into Eq. (13), it becomes

$$\begin{aligned}&\sum_{c=1}^{n+1} {}^b t_i^c \int_{-1}^{1} 2Re\left[\left[r_{ik}A_{jk}\log {}^b z_k\right]\right] N^c(\xi)J(\xi)d\xi \\ &= \sum_{c=1}^{n+1} {}^b t_i^c 2Re\left[\left[\int_{-1}^{1} r_{ik}A_{jk}\sum_{m=0}^{n}\alpha_m^{(c)}\xi^m \times \right.\right. \\ &\left.\left.\left[\log B_{nk} + \sum_{l=1}^{n}\log(\xi - R_{lk})\right]J(\xi)d\xi\right]\right]\end{aligned} \tag{17}$$

In Eq. (17), R_{mk} are roots of the polynomial equation

$$\frac{B_{0k} - ({}^b x_{p_1} + \mu_k {}^b x_{p_2})}{B_{nk}} + \sum_{m=1}^{n}\frac{B_{mk}\xi^m}{B_{nk}} = 0 \tag{18}$$

which can be solved using any convenient numerical scheme. Note that in Eq. (18), the coefficients are scaled by a common factor B_{nk}; this is to facilitate the solution for the roots of the equation. It serves also to distinguish the case of geometrically linear elements for which the factor is null and a separate algorithm may be employed; this is discussed later below. Under the nearly singular

condition when the source P approaches the integration element at the point$\xi = \xi_0$, it can be shown that one of the roots R_{mk} will approachξ_0. The weakly singular integral may be regularized by directly integrating Eq. (17) by parts, as follows. First, two functions, w and v, are introduced where

$$w(\xi) = \sum_{m=0}^{n} \alpha_m^{(c)} \xi^m J(\xi) \tag{19}$$

$$dv_k = \left[\log(B_{nk}) + \sum_{l=1}^{n} \log(\xi - R_{lk}) \right] d\xi \tag{20}$$

Thus, one may readily obtain

$$dw = \left[\sum_{m=1}^{n} m\alpha_m^{(c)} \xi^{m-1} J(\xi) + \sum_{m=1}^{n} \alpha_m^{(c)} \xi^m J'(\xi) \right] d\xi \tag{21}$$

$$v_k(\xi) = \xi \log(B_{nk}) + \sum_{l=1}^{n} (\xi - R_{lk}) \left[\log(\xi - R_{lk}) - 1 \right] \tag{22}$$

Equation (17) may now be rewritten as

$$\begin{aligned} &\sum_{c=1}^{n} {}^b t_i^c \int_{-1}^{1} 2Re \left[\left[r_{ik} A_{jk} \log {}^b z_k \right] \right] N^c(\xi) J(\xi) d\xi \\ &\quad = \sum_{c=1}^{n} {}^b t_i^c \, 2Re \left[\left[r_{ik} A_{jk} \left\{ \begin{array}{c} [w(\xi) v_k(\xi)]|_{-1}^{1} \\ -\int_{-1}^{1} v_k(\xi) \cdot \Omega^{(c)}(\xi) d\xi \end{array} \right\} \right] \right] \end{aligned} \tag{23}$$

In Eq. (23), the function $\Omega^{(c)}(\xi)$ is defined as

$$\begin{aligned} \Omega^{(c)}(\xi) &= \sum_{t=1}^{n} t\alpha_t^{(c)} \xi^{t-1} J(\xi) \\ &\quad + \frac{\sum_{t=0}^{n} \sum_{k=0}^{2n} \sum_{m=0}^{k} \sum_{j=0}^{n+1} \alpha_{n-m}^{(i)} \alpha_{n+m-k}^{(j)} \alpha_t^{(c)} x_l^{(i)} x_l^{(j)} \xi^{2n+t-k-3}}{2J(\xi)} \end{aligned} \tag{24}$$

In Eq. (24), the singular point R_{mk} in the original integrand of Eq. (17) is now removed through this regularization process. To illustrate the accuracy of this regularized formulation for the integral with the displacement kernel, consider the quadratic interpolation formulation (n=2) for a circular arc integration path with secant length D, as shown in Fig. 2. Suppose the source point lies at the mid-point of the arc with a distance L apart from it. For the purpose of demonstration here, the material constant μ_k and nodal coordinates can be arbitrarily chosen.

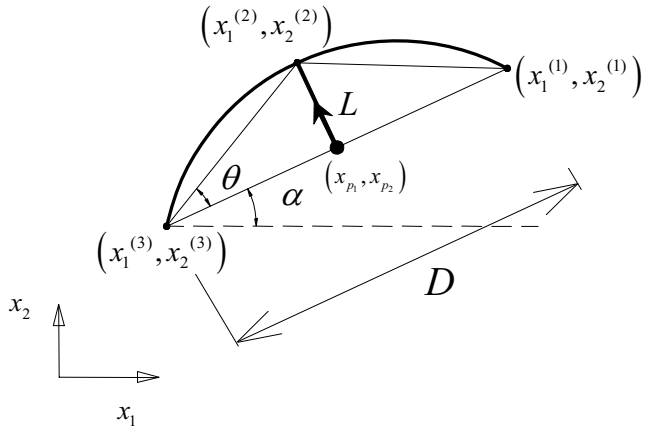

Figure 2 : A source point close to a quadratic element.

It is obvious that the integrand varies most rapidly for the case when c= 2, that is, when the value evaluated for the integral contributes to the coefficient in the equation matrix corresponding to the second node of the element. For this case, the variations of the integrands, in Eq. (17) and (23), are plotted in Fig. 3 for comparison. The very rapid variation near $\xi = 0$ when L/D is smaller than 10^{-2} will cause inaccurate evaluation of the integral by the usual simple numerical integration schemes. In contrast, the variation of the regularized integrand remains fairly slow and similar for any order of L/D.

The special case of when the elements used to model the physical problem are all straight is perhaps worth some discussion here. It is applicable to many practical problems with thin layers. In this situation, the coordinates of the m-th node are given by

$${}^b x_j^{(m)} = \frac{(m-1)^b x_j^{(n+1)} + (n-m+1)^b x_j^{(1)}}{n} \tag{25}$$

It can then be easily proved that the coordinates of an arbitrary point on element b are given by a simple form

$$\begin{aligned} {}^b x_j(\xi) &= \sum_{c=1}^{n+1} \sum_{m=0}^{n} \alpha_m^{(c)}(\xi) \xi^m \, {}^b x_j^{(c)} \\ &= \frac{\left({}^b x_j^{(n+1)} - {}^b x_j^{(1)} \right) \xi + \left({}^b x_j^{(n+1)} + {}^b x_j^{(1)} \right)}{2} \end{aligned} \tag{26}$$

Using Eq. (16), it may be readily shown that $B_{mk} = 0 \quad \text{for } m > 1$; this leads to

$${}^b z_k = C_{1k} \xi + D_{1k} \tag{27}$$

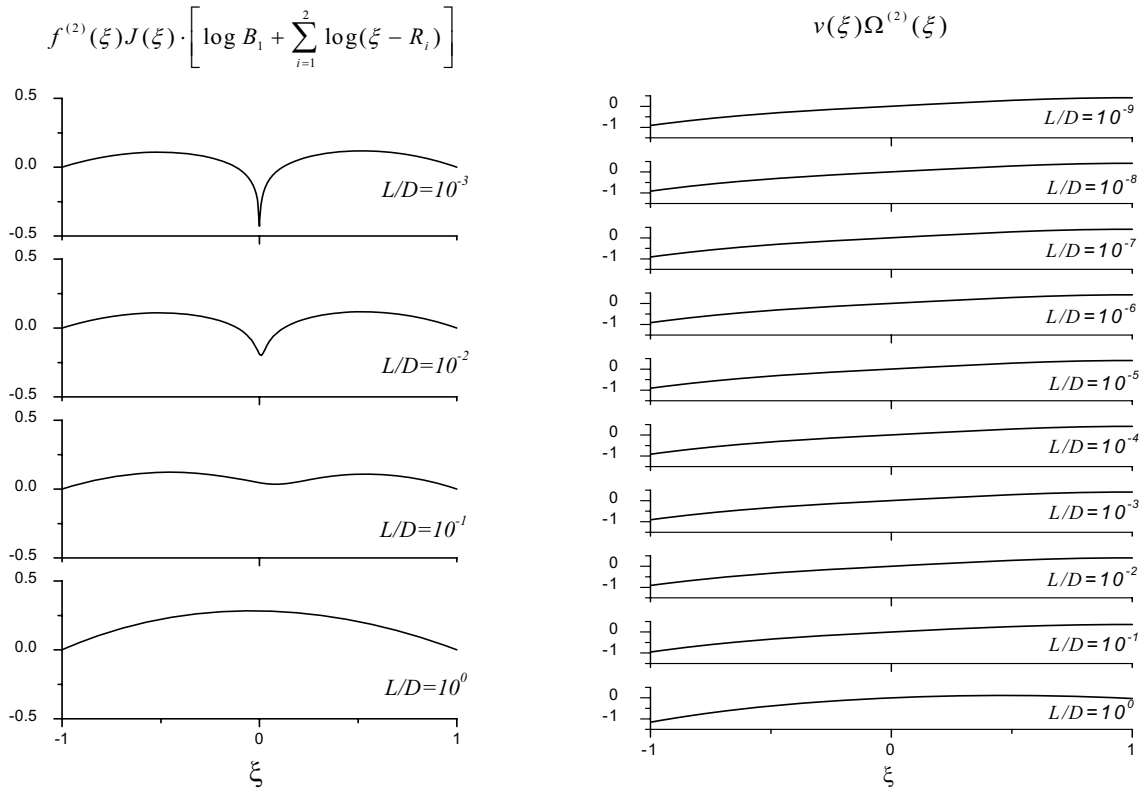

Figure 3 : Variations of the original and the regularized displacement kernels.

where the C_{1k}, D_{1k} are given by

$$C_{1k}=\frac{({}^bx_1^{(n+1)}+\mu_k{}^bx_2^{(n+1)})-({}^bx_1^{(1)}+\mu_k{}^bx_2^{(1)})}{2}$$
$$D_{1k}=\frac{({}^bx_1^{(n+1)}+\mu_k{}^bx_2^{(n+1)})+({}^bx_1^{(1)}+\mu_k{}^bx_2^{(1)})}{2}-(x_{p_1}+\mu_k x_{p_2}) \tag{28}$$

Also, the Jacobian is reduced to a simple form

$$J(\xi)=\sqrt{D_0} \tag{29}$$

where D_0 is given by

$$D_0=\frac{\left({}^bx_1^{(n+1)}-{}^bx_1^{(1)}\right)^2+\left({}^bx_2^{(n+1)}-{}^bx_2^{(1)}\right)^2}{4} \tag{30}$$

Using Eqs.(27) and (29) instead for the straight elements, Eq. (17) can now be rewritten as

$$\sum_{c=1}^{n+1}{}^bt_i^c\int_{-1}^{1}2Re\left[\left[r_{ik}A_{jk}\log{}^bz_k\right]\right]N^{(c)}(\xi)J(\xi)d\xi$$
$$=\sum_{c=1}^{n+1}{}^bt_i^c2Re\left[\left[\int_{-1}^{1}r_{ik}A_{jk}\sum_{m=0}^{n}\alpha_m^{(c)}\xi^m\left[\log C_{1k}+\log(\xi-R_{1k})\right]\sqrt{D_0}d\xi\right]\right] \tag{31}$$

where R_{1k} is given by

$$R_{1k}=D_{1k}/C_{1k} \tag{32}$$

By integrating the final form in Eq. (31) using the integration by parts successively, one may eventually have

$$\sum_{c=1}^{n+1}{}^bt_i^c\int_{-1}^{1}2Re\left[\left[r_{ik}A_{jk}\log{}^bz_k\right]\right]N^c(\xi)J(\xi)d\xi$$
$$=\sum_{c=1}^{n+1}{}^bt_i^c2\sqrt{D_0}Re\left[\left[r_{ik}A_{jk}\times\left[\begin{array}{l}\log C_{1k}\sum\limits_{m=0}^{n}\frac{\alpha_m^{(c)}}{m+1}\xi^{m+1}+\\ \sum\limits_{m=0}^{n}\sum\limits_{l=0}^{m}\frac{(-1)^l\alpha_m^{(c)}m!}{(m-l)!}\xi^{m-l}(\xi-R_{1k})^{l+1}\\ \left[E_{l+1}\log(\xi-R_{1k})-F_{l+1}\right]\end{array}\right]\Bigg|_{-1}^{1}\right]\right] \tag{33}$$

where the coefficients E_{n+1}, F_{n+1} are defined by the following recursive formulae

$$E_{l+1}=\frac{1}{(l+1)!},\quad F_{l+1}=\frac{F_l}{(l+1)}+\frac{E_l}{(l+1)^2},$$
$$(E_0=F_0=1) \tag{34}$$

Equation (33) is analytically exact for straight elements of any order. It should be reminded, however, this case can also be dealt with using the same algorithm of integration by parts as given by Eq. (23).

4 Treatment of the integral with the traction kernel

The fundamental solution for tractions (or traction kernel, for short) is $O(1/r)$, which is a stronger singularity than that of the displacements. It may therefore be expected that the previous process of integration by parts needs to be taken twice in principle so as to regularize the singular integral. The actual process may not be really necessary as will be shown below. As before, the expressions for ${}^b z_k(\xi)$ and $J(\xi)$ are given in Eqs. (14) and (15), respectively; the components of the unit outward normal vector are

$$n_1 = \frac{1}{J(\xi)} \sum_{c=1}^{n+1} \sum_{m=1}^{n} m \alpha_m^{(c)} \xi^{m-1} x_2^{(c)} \quad ,$$

$$n_2 = \frac{-1}{J(\xi)} \sum_{c=1}^{n+1} \sum_{m=1}^{n} m \alpha_m^{(c)} \xi^{m-1} x_1^{(c)} \tag{35}$$

By substituting Eqs. (13) and (35) into the integral with the traction kernel into Eq. (12), the result is

$$\begin{aligned}
&\sum_{c=1}^{n+1} \sum_{i=1}^{2} {}^b u_i^c \int_{-1}^{1} (-1)^{(i-1)} 2 \times \\
&\quad Re \left[\left[\mu_k^{\delta_{1i}} A_{jk} \left(\frac{n_1 \mu_k - n_2}{{}^b z_k} \right) \right] \right] N^{(c)}(\xi) J(\xi) d\xi \\
&\quad = \sum_{c=1}^{n+1} \sum_{i=1}^{2} {}^b u_i^c (-1)^{(i-1)} 2 \times \\
&\quad Re \left[\left[\begin{array}{l} \mu_k^{\delta_{1i}} A_{jk} \\ \int_{-1}^{1} \frac{\sum_{c=1}^{n+1} \sum_{m=1}^{n} m \alpha_m^{(c)} \xi^{m-1} \left(x_2^{(c)} \mu_k + x_1^{(c)} \right)}{\sum_{m=0}^{n} B_m \xi^m - ({}^b x_{p_1} + \mu_k {}^b x_{p_2})} \sum_{m=0}^{n} \alpha_m^{(c)} \xi^m d\xi \end{array} \right] \right] \\
&\quad = \sum_{c=1}^{n+1} \sum_{i=1}^{2} {}^b u_i^c (-1)^{(i-1)} 2 \times \\
&\quad Re \left[\left[\mu_k^{\delta_{1i}} A_{jk} \int_{-1}^{1} \sum_{j=1}^{n} \frac{G_{jk}^{(c)}}{\xi - R_{jk}} \sum_{m=0}^{n} \alpha_m^{(c)} \xi^m d\xi \right] \right]
\end{aligned} \tag{36}$$

where R_{jk}, again, are the roots of Eq. (18) and $G_{jk}^{(c)}$ are given by

$$G_{jk}^{(c)} = \frac{\sum_{c=1}^{n+1} \sum_{m=1}^{n} m \alpha_m^{(c)} R_{jk}^{m-n-1} \left(x_2^{(c)} \mu_k + x_1^{(c)} \right)}{B_{nk} \prod_{m=1}^{n} \left(1 - R_{mk}/R_{jk} + R_{mk} \delta_{mj} / R_{jk} \right)} \tag{37}$$

Equation (36) can be rearranged to give

$$\begin{aligned}
&\sum_{c=1}^{n+1} \sum_{i=1}^{2} {}^b u_i^c \int_{-1}^{1} (-1)^{(i-1)} 2 \times \\
&\quad Re \left[\left[\mu_k^{\delta_{1i}} A_{jk} \left(\frac{n_1 \mu_k - n_2}{{}^b z_k} \right) \right] \right] N^{(c)}(\xi) J(\xi) d\xi \\
&\quad = \sum_{c=1}^{n+1} \sum_{i=1}^{2} {}^b u_i^c (-1)^{(i-1)} 2 \times \\
&\quad Re \left[\left[\mu_k^{\delta_{1i}} A_{jk} \int_{-1}^{1} \sum_{j=1}^{n} \sum_{m=0}^{n} \alpha_m^{(c)} G_{jk}^{(c)} \right. \right. \\
&\quad \left. \left. \left(\frac{\xi^m - R_{jk}^m}{\xi - R_{jk}} + \frac{R_{jk}^m}{\xi - R_{jk}} \right) d\xi \right] \right] \\
&\quad = \sum_{c=1}^{n+1} \sum_{i=1}^{2} {}^b u_i^c (-1)^{(i-1)} 2 \times \\
&\quad Re \left[\left[\mu_k^{\delta_{1i}} A_{jk} \int_{-1}^{1} \sum_{j=1}^{n} \sum_{m=0}^{n} \alpha_m^{(c)} G_{jk}^{(c)} \right. \right. \\
&\quad \left. \left. \left(\sum_{l=1}^{m} \xi^{m-l} R_{jk}^{l-1} + \frac{R_{jk}^m}{\xi - R_{jk}} \right) d\xi \right] \right] \\
&\quad = \sum_{c=1}^{n+1} \sum_{i=1}^{2} {}^b u_i^c (-1)^{(i-1)} 2 \times \\
&\quad Re \left[\left[\mu_k^{\delta_{1i}} A_{jk} \sum_{j=1}^{n} \sum_{m=0}^{n} \alpha_m^{(c)} G_{jk}^{(c)} \right. \right. \\
&\quad \left. \left. \left(\sum_{l=0}^{m-1} \frac{R_{jk}^l \xi^{m-l}}{m-l} + R_{jk}^m \log(\xi - R_{jk}) \right) \right] \right] \Big|_{-1}^{1}
\end{aligned} \tag{38}$$

which is analytically exact for elements of any order. That being true, it should be noted that Eq. (38) can be considered as only a "semi-analytical" formulation since the determination of the roots, R_{jk}, in general, requires a numerical scheme. However, if quadratic elements (n=2), which are the most commonly adopted ones employed in BEM analysis, the formulation is indeed analytically exact. This is because the corresponding two roots can be analytically determined from its second order polynomial equation. For geometrically straight ele-

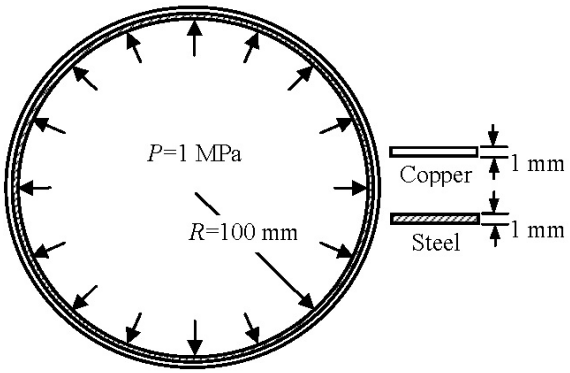

Figure 4 : A bimetallic cylindrical ring subjected to internal pressure.

ments, there exist only one root (l=1), i.e. R_{1k}as given by Eq. (32).

5 Numerical examples

To demonstrate the veracity of the formulations proposed above, three numerical examples are presented here. The first one is a bi-metallic cylindrical ring as shown in Fig. 4; it consists of steel cylindrical ring (Young's modulus E = 207 GPa, Poisson's ratio ν = 0.3) neat-fitted into a copper ring (Young's modulus E = 117.7 GPa, Poisson's ratio ν = 0.33) and under internal pressure of P=1 MPa. Although the problem is isotropic, it is solved using the BEM algorithm for anisotropy by small perturbations of the isotropic properties. This problem is chosen as a quick check of the successful implementation of the proposed formulations, as the exact analytical solution (Lame's solution) exists. Taking advantage of symmetry, only one-quarter of the physical domain is modeled with the appropriate displacement constraints applied along the planes of symmetry. Figure 5 shows the typical BEM mesh employed when the circumferential surfaces are discretised into 4 elements (N=4), while only one element is used in the through-thickness direction for each layer. The BEM computed hoop stress at the nodes along each circumferential surface is uniform, as expected; these stresses are listed in Table 1 together with the exact theoretical value according to Lame's solution. It can be seen that even with the relatively coarse meshes used in the analysis, very high accuracy of the BEM solutions is achieved.

For the second example, a printed circuit board (PCB) used in electronic applications is considered. It is a 9-

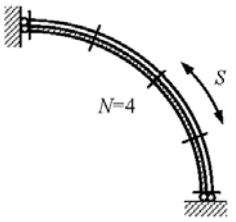

Figure 5 : BEM model of Example 1.

Table 1 : Hoop stresses (in MPa) along the circumferential surfaces of the bi-metallic rings – Example 1

N	S/D	Steel			
		Inside Surface		Outside surface	
		64.27	Err. %	63.63	Err. %
4	40.06	63.40	1.35	62.81	1.29
8	20.03	63.83	0.68	63.23	0.63
10	16.02	63.87	0.62	63.23	0.63
N	S/D	Copper			
		Inside Surface		Outside surface	
		36.23	Err. %	35.88	Err. %
4	40.06	36.38	0.41	36.05	0.47
8	20.03	36.63	1.09	36.29	1.13
10	16.02	36.62	1.08	36.26	1.05

N: The number of discretised elements over the circumferential arc

D: The thickness of the outside layer (1 mm)

S: The arc length of each element of the modeled outside copper wall

ply symmetric laminate, as shown in Fig.6, comprising of layers of solder mask, FR-4 composite, and copper. The thickness of each layer and the length of the plate analysed are as indicated in the figure. The board is subjected to uniaxial tension P=1 MPa at the remote ends. The mechanical properties of the constituent layers in the plane considered in the BEM analysis are listed in Table 2, NEC(Taiwan) (2005); the other mechanical properties of anisotropic FR4 that are not listed in the table, namely, the coefficients of mutual influence and Chentsov's coefficient, are zero. Only one-quarter of the problem is modeled as shown in Fig. 7(a) because of the geomet-

Table 2 : Mechanical properties of the constituent materials for the printed circuit board –Example 2

Material	Young's modulus	Poisson's ratio	Shear Modulus
Solder mask	E=1.96 *GPa*	ν = 0.35	G=0.73 *GPa*
Cu	E=117.68 *GPa*	ν = 0.33	G=44.24 *GPa*
FR-4	E_{11}=E_{33}=16.85 *GPa* E_{22}=7.38 *GPa*	ν_{12} = ν_{23} = 0.11 ν_{13} = 0.39	G_{12}=G_{23}= 3.29 *GPa* G_{13}=6.95 *GPa*

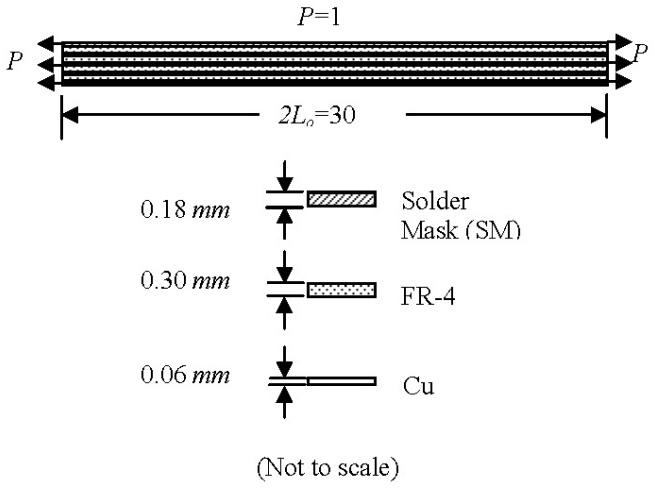

Figure 6 : Example 2 - A printed circuit board (PCB) under remote uniaxial tension.

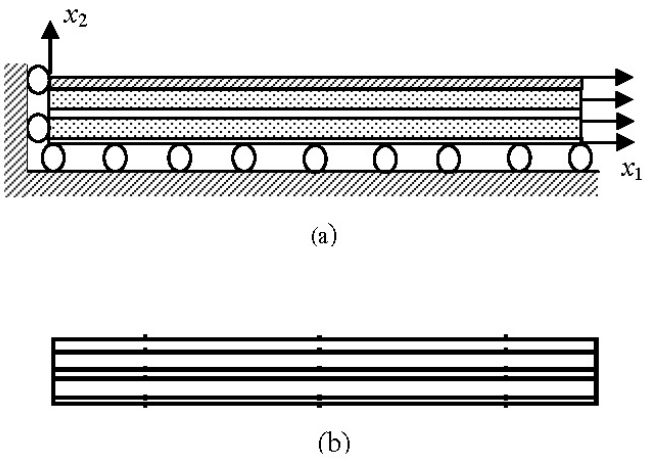

Figure 7 : (a) A quarter model of Example 2. (b) BEM mesh of Example 2.

ric and material symmetry in the plane shown in Fig. 6, and plane strain conditions are assumed. Figure 7(b) shows the BEM mesh employed; it has a total of only 50 quadratic elements (n=2) for the modeling of all 5 subregions of the layers. As a means of verification of the numerical results, this problem is also solved using the finite element method (FEM) with the commercial code ANSYS. Due to the thinness of the elements and to ensure reasonable aspect ratios of their side lengths, 28000 PLANE42 (linear) elements are employed. Because of this high density of elements, the FEM mesh is not presented here. As expected, the computed normal stresses $\sigma_{22}$and σ_{12} throughout all layers are very small that can be neglected. The computed values of$\sigma_{11}$are found, for all intents and purposes, to be uniform but distinct in each different constituent material; their values at the interfaces for the respective materials are shown in Fig.8 for both the BEM and FEM analyses. For the sake of clarity, the results at $x_1/L_o = 1$ where the external load is applied, are not shown because of the stress discontinuities at the interfaces. Excellent agreement of the numerical results from both analyses can be seen; the discrepancies in the vicinity of the ends are due to the discontinuities in the stresses there.

The third example treated here is a lap-joint shown in Fig. 9 with plates of FR4 bonded by an epoxy adhesive (Young's modulus, E=3GPa, and Poisson's ratio, ν= 0.38) under remote uniform tensile stress. The dimensions considered are as indicated in the figure. By virtue of symmetry, only one-half of the physical domain is modeled, and plane strain conditions are assumed. Figure 10 shows the BEM mesh with a total of 50 quadratic elements employed for the three sub-regions of the three modeled layers. An FEM analysis using ANSYS is also carried out in which 5114 PLANE42 (linear) elements are used; the mesh is again not shown here because of the high density of the elements used. The distributions of the boundary stresses, uniform in each respective layer, are shown in Fig.11, 12, and 13 for the central plate, the adhesive, and the outer plate, respectively. In these figures, the stresses are shown as a function of the

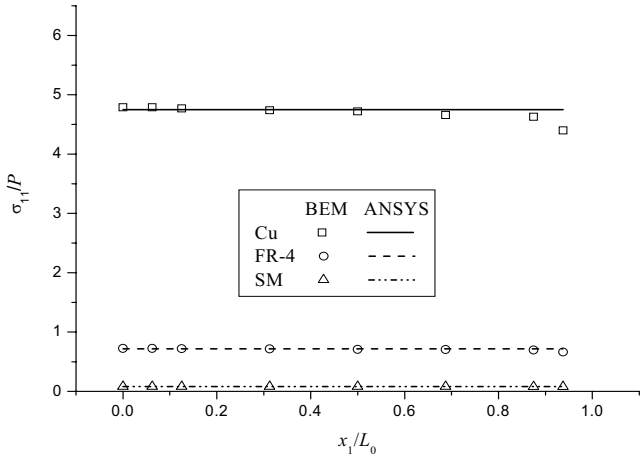

Figure 8 : Distribution of the normalized stress,σ_{11}/P, in the constituent layers - Example 2.

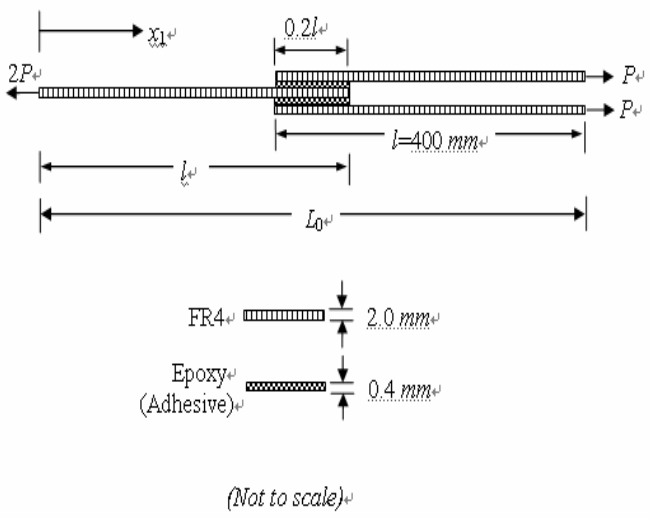

Figure 9 : Example 3 - An FR4 lap-joint in remote tension.

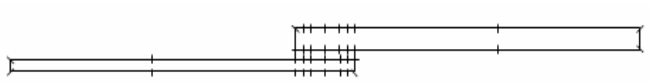

Figure 10 : BEM mesh for Example 3.

non-dimensional distance x_1/L_0, where L_0 is the overall length of the lap-joint as defined in Fig.9. Since the stress component σ_{22} is negligible in all three layers, they are not shown here. As can be seen from these figures, even with a relatively coarse rough mesh, the BEM results are still in very satisfactory agreement indeed with those obtained from the more refined FEM analysis. It is perhaps

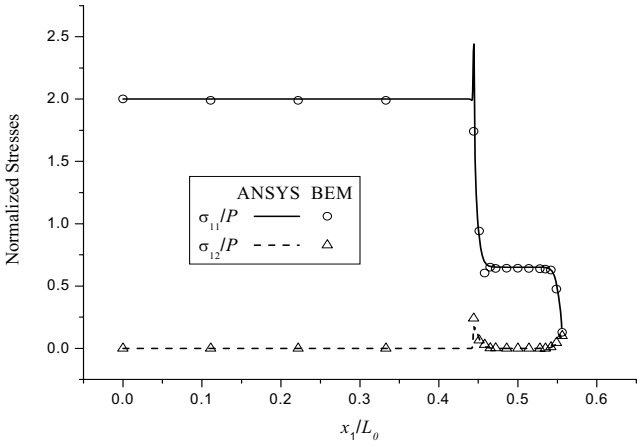

Figure 11 : Distribution of the normalised stresses, σ_{11}/P and σ_{12}/P, in the central plate- Example 3.

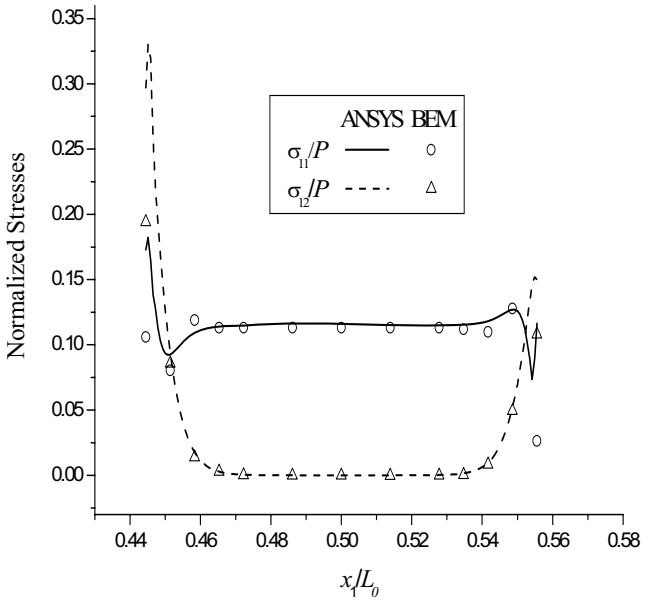

Figure 12 : Distribution of the normalised stresses, σ_{11}/P and σ_{12}/P, in the adhesive- Example 3.

worth noting that at the corner edges of the adhesive, the stresses are singular; the discrepancies between the results from the two numerical methods which are more evident there are thus to be expected.

6 Conclusions

The fundamental solutions to the governing equations which are employed in the formulation of BEM analysis are singular and they form the integrands of the boundary

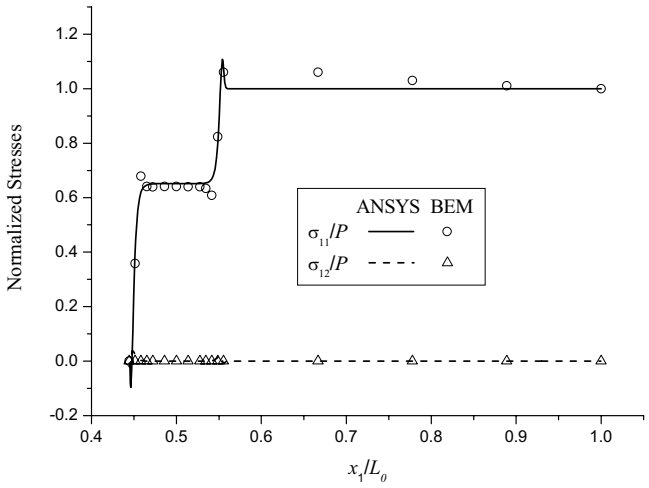

Figure 13 : Distribution of the normalised stresses, σ_{11}/P and σ_{12}/P, in the outer plate - Example 3.

integral equation (BIE). Nearly singular integrals arise when performing analysis of, for example, thin, slender bodies, and accurate evaluations of these integrals pose a challenge in conventional BEM analysis. In this paper, the regularization of the integrands appearing in the BIE for two-dimensional anisotropic elasticity has been carried out using integration by parts. An expression for the exact evaluation of the integral containing the traction fundamental solution over a general element of *n*-order interpolation of the variables has been derived. This has allowed thin, slender, anisotropic, elastic bodies to be modeled without the need for very refined meshes in the BEM analysis. Three example problems involving thin, layered materials have been presented in this paper; the BEM results have been compared with the exact analytical solution for one and with those from the FEM analysis of the same problems in the other two. It has been shown that accurate BEM solutions were obtained for these problems even with relatively coarse mesh designs. Although it is not an aim of the present paper, the application of the BEM code developed to the study of the singular stresses at some points in the numerical examples shown would also be useful when the determination of the damage initiation and its growth in the geometries are of interest.

Acknowledgement: The financial support received by Y.C. Shiah and Y.C. Lin from the National Science Council of Taiwan (Grant No. NSC94-2212-E-035-011) is gratefully acknowledged.

References

Cruse, T.A.; Aithal, R. (1993): Non-singular boundary integral equation implementation, *Int. J. Numer. Methods Engng.*, 36, 237-254.

Dominguez, J.; Ariza, M.P.; Gallego, R. (2000): Flux and traction boundary elements without hypersingular or strongly singular integrals, *Int. J. Numer. Methods Engng.*, 48, 111-135.

Dumont, N.A. (1994): On the efficient numerical evaluation of integrals with complex singularity poles, *Engng. Anal. Boundary Elements*, 13, 155-168.

Granados, J.J. and Gallego, R. (2001): Regularization of nearly singular integrals in the boundary element method, *Engng. Anal. Boundary Elements*, 25, 165-184.

Hayami, K. (1992): *A Projection Transformation Method for Nearly Singular Surface Boundary Element Integrals*, Lecture Notes in Engineering, **73**, Brebbia, C.A. and Orszag, S.A. (eds.), Springer-Verlag, Berlin.

Hayami, K.; Matsumoto, H. (1994): Numerical quadrature for nearly singular boundary element integrals, *Engng. Anal. Boundary Elements*, 13, 143-154.

Huang, Q.; Cruse, T.A. (1993): Some notes on singular integral techniques in boundary element analysis, *Int. J. Numer. Methods Engng*. 36, 2643-2659.

Jun, L., Beer, G.; Meek, J.L. (1985): Efficient evaluation of integrals of order 1/r, $1/r^2$, $1/r^3$ using Gauss quadrature, Engng. Anal. *Boundary Elements*, 2, 118-123.

Kant, T.; Swaminathan, K. (2000): Estimation of transverse/interlaminar stresses in laminated composites- a selective review and survey of current developments, *J. Composites*, 49, 65-75.

Krishnasamy, G.; Rizzo, F.J.; Liu, Y.J. (1991): Boundary integral equation for thin bodies, *Int. J. Num. Methods Engng.*, 37, 107-121.

Lekhnitskii, S.G.(1963): *Theory of Elasticity of an Anisotropic Body*, Holden-Day.

Liu, Y.J., Zhang, D. and Rizzo, F.J.(1993): Nearly singular and hypersingular integrals in the boundary element method, in Boundary Elements XV, Vol. 1, Brebbia, C.A. and Rencis J.J. (eds.), Computational Mechanics Pub., U.K., 453-468.

Lutz, E.D. (1992): Exact Gaussian quadrature methods for nearly singular integrals in the boundary element method, *Engng. Anal. Boundary Elements*, 9, 233-245.

Lutz, E.D.; Gray, L.J.; Ingraffea, A.R. (1991): An overview of integration methods for hypersingular boundary integrals, in *Boundary Elements XIII*, Brebbia, C.A. and Gipson, G.S. (eds.), Computaional Mechanics Pub., U.K., pp. 913-925.

Lutz, E.D.; Gray, L.J. (1993): Analytic evaluation of singular boundary integrals without CPV, *Comm. Numer. Methods Engng.*, 9, 909-915.

Martin, P.A.; Rizzo, F.J.; Cruse, T.A. (1998): Smoothness relaxation strategies for singular and hypersingular integral equations, *Int. J. Numer. Methods Engng.*, 42, 885-906.

Mi, Y.; Aliabadi, M.H. (1996): A Taylor expansion algorithm for integration of 3D near-hypersingular integrals, *Comm. Numer. Methods Engng.*, 12, 51-62, 1996.

Nakagawa, N. (1993): Near-surface field evaluation in two-phase Helmholtz problem, IABEM-93 Symposium, Braunschweig, Germany.

NEC (Taiwan), *Private communication.*

Pagano, N.J.; Hatfield, S.J. (1972): Elastic behavior of multi-layered bi-directional composites, *AIAA*, 10, 931-933.

Richardson J.D. and Cruse, T.A. (1999): Weakly-singular stress-BEM for 2D elastostatics, *Int. J. Numer. Methods Engng.*, 45, 13–35.

Rosen, D.; Cormack, D.E. (1994): The continuation approach for singular and near-singular integration, *Engng. Anal. Boundary Elem.*, 13, 99-113.

Sladek, V. and Sladek, J. (1992): Non-singular boundary integral representation of stresses, *Int. J. Numer. Methods Engng.*, 33, 1481-1499.

Tanaka, M.; Sladek, V.; Sladek, J. (1994): Regularization techniques applied to boundary element methods, *Appl. Mech. Rev.*, 47, 457-499.

Telles, J. (1987): A self-adaptive coordinate transformation for efficient numerical evaluation of general boundary element integrals, *Int. J. Numer. Methods Engng.*, 24, 959-973.

Wu, S. and Lu, P.A. (1996): On the evaluation of nearly singular kernel integrals in boundary element analysis – some improved formulations, *Comm. Numer. Methods Engng.*, 12, 85-93.